Single-Molecule Super-Resolution Microscopy Reveals Formation of NS2B3 Protein Clusters on Mitochondrial Network Leading to its Fragmentation during the Onset of Dengue (Denv-2) Viral Infection

Jiby M. Varghese†, Prakash Joshi†, Aravinth S, and Partha P. Mondal
Department of Instrumentation and Applied Physics, Indian Institute of Science, Bangalore 560012, INDIA
(Dated: June 28, 2023)

NS2B3 is a key protein complex essential for proteolytic activity and processing of viral polyprotein during dengue type 2 (Denv-2) infection. The underlying mechanism involved in the early onset (first 48 hrs) of dengue pathogenesis was studied using single molecule-based super-resolution microscopy to understand the Denv-2 infection. The study was conducted on NIH3T3 cells transfected by two distinct photoactivable fusion plasmid DNAs ($mEos3.2 - NS2B3$ and $PAGFP - NS2B3$). Studies demonstrated that the formation of NS2B3 clusters on the mitochondrial network induces its fragmentation. The NS2B3 complex acts as a protease that clips specific sites of mitofusin (MFN1/2) proteins, responsible for fusion which holds the network together, disrupting the mitochondrial network. Statistical analysis of super-resolution data (images) estimates an average NS2B3 cluster area of $\approx 0.050\ \mu m^2$ with a density of $\approx 3500 mol./\mu m^2$, and an average of ≈ 120 molecules per cluster. Based on the present study, we hypothesize that the formation of clusters and the associated cluster-related parameters are critical in promoting mitochondrial fragmentation. Overall, the single molecule-based super-resolution study helped reveal the basic mechanism of single-molecule (NS2B3) clustering during the onset of dengue viral infection. Understanding the underlying biophysical mechanism of NS2B3 clustering at the single molecule level may help decipher potential drug targets and the mechanisms of action to disrupt the NS2B3 clusters, which may ultimately usher the way to contain/treat dengue viral infection.

Statement of Significance: The arrival of single molecule based super-resolution microscopy techniques have advanced the field of cell biology, and our understanding of sub-cellular processes with single molecule precision. Here, we report the first ever application of super-resolution microscopy to visualize NS2B3 clusters that lead to the fragmentation of mitochondrial network. To facilitate this study, two new photoactivable probes ($mEos3.2 - NS2B3$ and $PAGFP - NS2B3$) with key protein complex, NS2B3 of dengue virus were developed. The study involves cell transfection studies and single molecule imaging. The proposed study is expected to decipher potential drug candidates and the mechanisms of action to disrupt the NS2B3 clusters, which may ultimately usher the way to contain/treat dengue viral infection.

Corresponding author (Partha Pratim Mondal): partha@iisc.ac.in
†First two authors contribute equally to this work.

I. INTRODUCTION

Dengue virus is an enveloped virus that consists of capsid protein (C) and a positive single-stranded RNA molecule. The dengue genome encodes a polyprotein which ultimately produces ten proteins after cellular processing, of which three structured proteins (C, prM/M, E) and seven non-structured proteins (NS1, NS2A, NS2B, NS3, NS4A, NS4B, and NS5) [1]. Out of these proteins, it is the non-structural proteins that are directly involved in viral replication and assembly [1] [2] [3] [4] [5]. NS2B, a non-structural protease sub-unit, promotes conformational changes in the NS3 structure [6] [7] [8]. Specifically, NS3 protein has the distinct ability to cleave parts of polyprotein precursor and is actively involved in viral replication due to its ATPase/helicase and RNA triphosphatase domain in the C-terminal region [9] [10] [11]. Together, NS2B/NS3 (in short, NS2B3) is a highly conserved protein and forms a weak non-covalent complex. The NS2B3 complex is responsible for proteolytic activity and processing of viral polyprotein at the junctions with other non-structured proteins (NS2B-NS3, NS2A-NS2B, NS3-NS4A, NS4B-NS5) [12] [13]. The NS2B-NS3 protease is crucial in correctly processing viral polyproteins during dengue viral infection.

Like most flaviviruses, dengue virus uses the host cellular mechanism to multiply and infect other healthy cells [1] [14]. However, little is known about what transpires at the single molecule level, their interactions, and their distribution during infection. Such information is vital to understand the underlying mechanism and selective drug targets to disrupt the onset of these processes, hoping to inhibit the chain of viral infection.

Studies over the years suggest that the NS2B3 protein complex interacts with several cellular proteins, which is essential for effective infection of dengue virus to host cell [15] [16] [17]. Dengue infection begins with virion E protein binding to the host cell surface ligands [18]. The dengue virus, up on receptor-mediated endocytosis, releases viral RNA genome into host cytosol and starts producing single viral polyprotein [19]. The polyprotein using host cellular machinery produces ten vital viral structural and non-structural proteins. In conjunction with host cellular proteins, the viral proteins facilitate RNA replication, budding, and complete virion maturation [20]. Dengue virion utilizes all the host organelles involved in protein expression to maturation. At the endoplasmic reticulum (ER) membrane, the NS3 protein interacts with fatty acid synthase resulting in enhanced fatty acid biosynthesis, which increases virion packaging [21]. The virion matures in the Golgi bodies, and the Golgi network helps it release into the extracellular region [22] [23].

Recent studies reported that NS2B3 protease targets host mitochondria, which induces matrix-localized GrpE protein homolog 1 (GrpEL1) cleavage. The GrpEL1 protein, a cochaperone of the Hsp-70 protein, cleavage led to the dysfunction of the Hsp-70 protein, hampering overall protein folding. Thus, GrpE1 cleavage leads to mitochondria and mitochondrial-associated membranes (MAMs) disruption and mitofusins (MFN1 and MFN2), causing mitochondrial fragmentation [24]. NS2B3 proteases induce mitochondrial disruption responsible for inducing apoptosis in human medulloblastoma cells. It also blocks RIG-1 and MDA-5 translocation to the mitochondria from the cytosol leading to suppression of the host immune response [25]. However, the exact consequences of NS2B3 protease dysfunction at the molecular level are yet to be studied. Here we studied the interaction of NS2B3 protease with the mitochondrial matrix and evaluated its fragmentation mechanism at the single-molecule level. Most existing studies are performed by diffraction-limited microscopy techniques that are known to give ensemble information. Hence, the dynamics and related kinetics at a single molecule or cluster level were never revealed.

Over the last few decades, the disease biology of dengue has advanced substantially with the advance of modern microscopes and biomolecular analysis. Mitochondrial damage due to dengue infection is revealed in confocal microscopy as reported by many researchers [26] [37] [38] [39]. Dengue protease, NS2B3 interferes with mitochondrial fusion and mitochondrial dynamics by cleaving mitochondrial outer membrane protein mitofusin 1 and mitofusin 2 (MFN1/2) [26]. Specifically, mitofusins help in mitochondrial fusion by tethering adjacent mitochondria [27], and decreased mitofusin activity leads to mitochondrial fragmentation [28]. It is found that MFN1 positively regulates host antiviral signaling, and MFN2 is responsible for mitochondrial membrane potential during dengue infection [29]. The cleavage of both MFNs by dengue protease would attenuate interferon production and promotes dengue-induced cell death [26]. But still, it is not well known about the mode of attachment of NS2B3 protease complex on mitochondrial membrane and its fate after attachment. There is no information available

at the single molecule level and thus, the underlying mechanism is unknown. It requires sophisticated super-resolution microscopy and single-molecule-based biological protocols. A better understanding of the infection process may lead to precision drug targeting and selective therapy for the disease.

This report presents the dengue (type 2) infection mechanism at a single molecule level for the first time using single-molecule localization microscopy (SMLM). SMLM has advantages as compared to other super-resolution microscopes (such as STED, structured illumination, and its recent variants) for quantifying individual molecules and their collective dynamics. These viral proteins are known to undergo processes such as migration, cluster formation, and localization to the specific organelle. Understanding these processes paves the way to effective therapy for diseases where single molecule-based super-resolution techniques play a pivotal role. Here, we study the dynamics of NS2B3 complex mechanism of action post-entry in the cellular system. We investigate the collective dynamics of single molecules by suitably fusing the NS2B3 protein with a photoactivable protein. Studying the NS2B3 interaction mechanism at the molecular level has allowed us to decipher processes both at the single-molecule and cluster levels. Related biophysical parameters (cluster size, density, and copy number) related to the viral protein complex are critical in assessing the progress of the Denv-2 infection process.

II. RESULTS

In the present study, we investigate the role of NS2B3 complex post-entry to the host cell. To accomplish this, we need appropriate fluorescent probes in order to localize the site or organelle of activity. Two photoactivable probes are designed: PAGFP-NS2B3 and mEos-NS2B3. The presence of NS2B3 fragment in PAGFP-NS2B3 was confirmed by PCR and restriction digestion analysis. PCR of PAGFP-NS2B3 using NS2B3-specific primers gave an amplicon around 2300bp and restriction analysis using the restriction enzyme pair Pst 1 and Bam H1 released a fragment of 2300 bp along with 1Kb ladder. Similarly, PCR of mEos-NS2B3 using mEos-specific primers gave an amplicon around 700 bp along with 1 Kb ladder confirming the presence of mEos fragment in recombinant vector. The recombinant nature of both PAGFP-NS2B3 and mEos-NS2B3 was further confirmed by sequencing. Sequence analysis confirmed the intactness of the reading frame while fusing NS2B3 with the fluorophore (PAGFP/mEos). Results of PCR, restriction analysis and sequencing along with recombinant vector map were given in **Supplementary 1-3**.

The recombinant plasmids, both PAGFP-NS2B3, and mEos-NS2B3 were used to transfect NIH3T3 cells (mouse embryonic fibroblast cell line) to study the interaction of dengue NS2B3 with the cellular organelles.

Fig.1 shows NIH3T3 cells transfected with PAGFP-NS2B3 / mEos-NS2B3 (individual transfections) recombinant plasmids DNA followed by the standard protocol of washing, culture, and incubation for 48 hrs. As a control, cells were also transfected by a standard Dendra2-Tom20 plasmid in a separate experiment. The transfection was confirmed by exposing it to blue light and observing the fluorescence in green. It is clear that PAGFP-NS2B3 / mEos-NS2B3 protein complex is expressed and located on the mitochondrial membrane. This can be ascertained by the control experiment where a known and targeted protein Dendra2-Tom20 is expressed on mitochondrial membrane [35] [36]. A few enlarged images of individual cells are also shown in Fig. 1. To ascertain the presence of PAGFP-NS2B3 / mEos-NS2B3 protein complex on the mitocondrial network, we have carried out colocalization studies. The experiment involves transfecting NIH3T3 cells with mEos-NS2B3 recombinant plasmid. Upon expression of the mEos-NS2B3 recombinant protein, the cells were washed and labeled with MitoTracker orange (Invitrogen, USA). The specimen is then fixed following standard protocol and imaged using confocal microscopy, as shown in Fig. 2. It is evident that mEos-NS2B3 recombinant protein and MitoTracker orange show a high degree of colocalization. This can be visually confirmed from the merged images (see Fig.2A) and the enlarged section (R1 and R2). The corresponding statistical analysis based on Pearson's coefficient ($\eta = 0.8422$) and overlap coefficient ($\gamma = 0.9139$) further confirms strong colocalization of mEos-NS2B3 and MitoTracker orange. A similar experiment is repeated with PAGFP-NS2B3 plasmid as shown in Fig.2B. Again, colocalization of PAGFP-NS2B3 protein and MitoTracker orange demonstrate strong colocalization both visually (see Fig.2B, merged and enlarged images) and statistical analysis ($\eta = 0.8332$ and $\gamma = 0.8436$). A control experiment was performed with with dendra2 Tom20 plasmid as shown in Fig.2C. The colocalization of dendra2-Tom20 protein and MitoTracker orange demonstrate strong colocalization, visually (Fig.2C, merged and enlarged images) and based on statistical analysis ($\eta = 0.8231$ and $\gamma = 0.8337$). We have also determined mitochondrial fragment length (mitochondrial labeled with MitoTracker orange) to be 495.9 ± 12.30 nm and 601.2 ± 11.79 nm for $mEos - NS2B3$ and $PAGFP{-}NS2B3$, respectively. However, the mitochondrial fragment length of dendra2-Tom20 transfected cells appears to be longer (853.1 $\pm$ 14.70) indicating a relatively unfragmented mitochondrial network. Overall, these experiments confirm the location of the viral complex $NS2B3$ on the mitochondrial network, establishing mitochondria as its target organelle during the onset of Denv-2 viral infection (post 48 hours post transfection). There are also enough evidences that suggests transfected NS2B3 mimic actual NS2B3 function during dengue infection [24] [26].

The next step is to probe and analyze the confocal images to assess the effect of PAGFP-NS2B3 / mEos-NS2B3 protein complex on the mitochondrial network. Image-based analysis of mitochondrial morphology is standard for analyzing mitochondrial fragment characteristics [48] [49] [54]. We have used Dendra2-Tom20 transfected cells as a control experiment to understand mitochondrial function which is a common practice for super-resolution studies, as evidenced in literature [50] [51] [52]. Moreover, studies have shown that over-expression of Dendra2-Tom20 did not affect mitocondria [53]. So, we have used Tom20 as a mitochondrial marker for the control experiment. Fig. 3 shows mitochondrial network for PAGFP-NS2B3 / mEos-NS2B3 transfected cell and the control experiment (Dendra2-Tom20 transfected cells). The acquired images are subjected to edge-detection using standard inbuilt Matlab scripts, as shown in Fig. 3. Visually, the presence of small segments is evident suggesting fragmentation of mitochondrial network in PAGFP-NS2B3 / mEos-NS2B3 transfected cells. This can be further confirmed by comparing it with a control experiment that shows a long-connected mitochondrial network. To quantize, we carried out statistical analysis related to segment size histogram, number of fragments, and image entropy. Segment size analysis clearly indicates the presence of shorter segments for PAGFP-NS2B3 (average size, $464.4 \pm 15.30nm$) and mEos-NS2B3 (average size 545.4 ± 8.50 nm) transfected cells as compared to control (average size, $866.6 \pm 24.35nm$). This confirms the breakdown of the mitochondrial network by the viral complex NS2B3. In addition, the number of segments has increased by more than 2-fold for NS2B3 transfected cells (see, Fig. 3D). Moreover, we have used the Shannon entropy measure to assess randomness (distribution of fragments) in each case. For control, Dendra2-Tom20 transfected cells were expected to preserve the connectedness in the mitochondrial network, which is quite evident for control suggesting low entropy. On the other hand, PAGFP-NS2B3 and mEos-NS2B3 transfected cells show relatively high entropy. The corresponding significance values less than 0.05 indicate that the observed difference is unlikely by chance and is highly significant compared to the control. The area of interest for all the images was kept constant while calculating the entropy. The analysis shows that PAGFP-NS2B3 is more random among the other two plasmids, where Dendra2-Tom20 being the minimum. This also indicates that Dendra2-Tom20 has more network connectivity than the recombinant plasmids. Clearly, the confocal experiments show short segments of the randomly-distributed mitochondrial network brought about by the viral complex NS2B3.

The existing diffraction-limited optical microscopy techniques are often inadequate to visualize molecular clusters, primarily due to their limited resolution. This severely limits a deeper understanding of the biology of viral infection, specifically at the molecular scale.

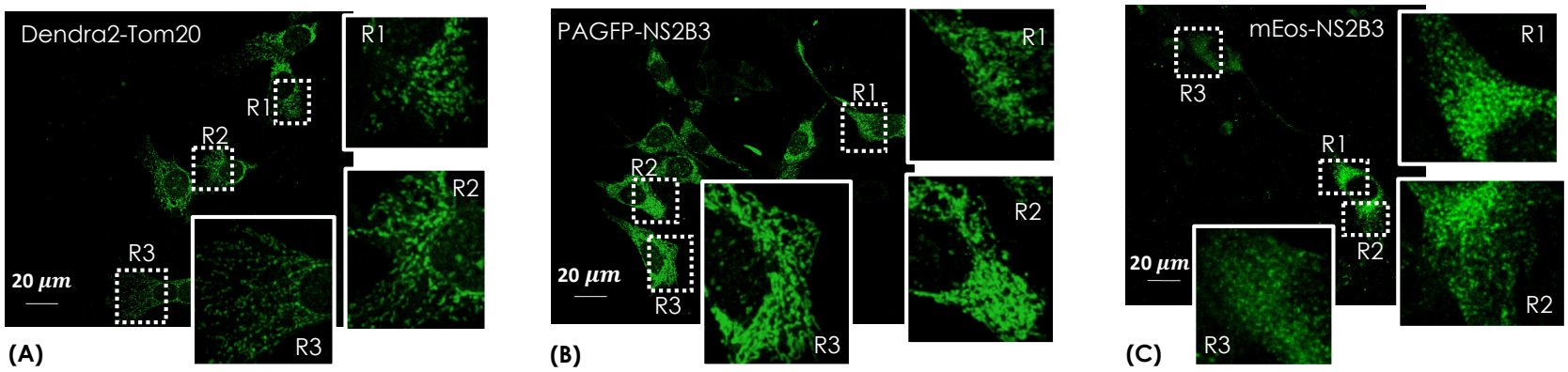

FIG. 1: **Transfection studies of NS2B3 using confocal microscopy:** (A) NIH3T3 cells expressing Dendra2-Tom20 protein. (B,C) Transfected NIH3T3 cells show localization of complex viral proteins, $PAGFP - NS2B3$ and $mEos - NS2B3$. Few enlarged sections (R1, R2 and R3) are also shown.

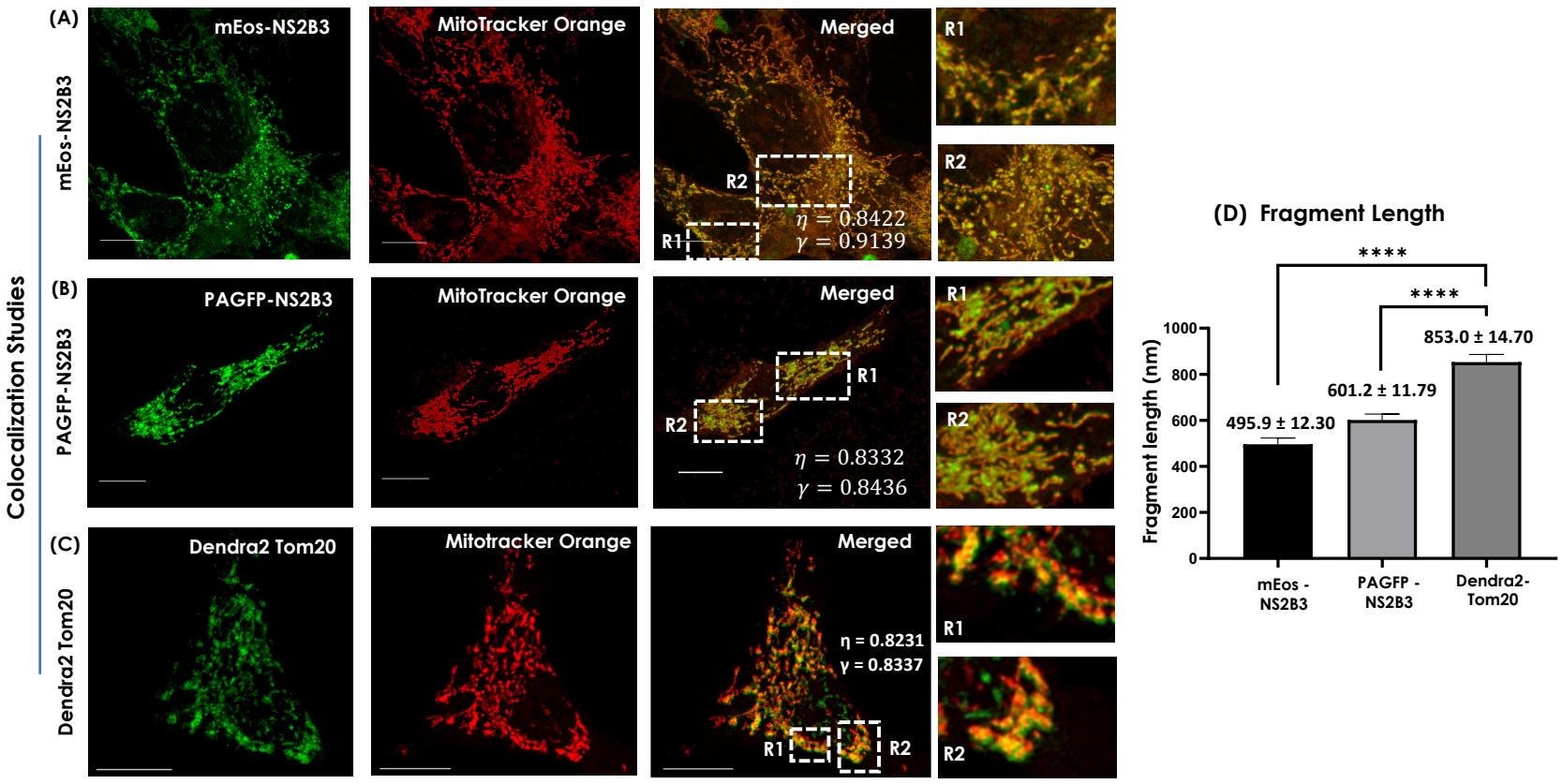

FIG. 2: **Confocal microscopy studies shows the colocalization of Dengue NS2B3 protease and mitochondria :** (A) Fluorescence images of mEos-NS2B3 transfected NIH3T3 cells labelled with MitoTracker Orange dye, along with the merged image (Pearson's coeff (η) = 0.8422; Overlap coefficient ($\gamma = 0.9139$)). (B) Fluorescence images of PAGFP-NS2B3 transfected NIH3T3 cells labelled with MitoTracker Orange dye, along with the merged image ($\eta = 0.8332$; $\gamma = 0.8436$)). Few enlarged sections (R1, R2 and R3) are also shown. (C) Fluorescence images of Dendra2-Tom20 transfected NIH3T3 cells labelled with MitoTracker Orange dye, along with the merged image ($\eta = 0.8231$; $\gamma = 0.8337$). Few enlarged sections (R1, R2 and R3) are also shown. (D) The corresponding plots gives histogram of the length of fragmented mitochondria. Mitochondrial fragment lengths presented here are calculated based on 15 cells from 3 different experiments for both PAGFP-NS2B3 and mEos-NS2B3. We have determined mitochondrial fragment length (mitochondria labeled with mitochondrial orange) to be 495.9 ± 12.30 nm and 601.2 ± 11.79 nm for mEos-NS2B3 and PAGFP-NS2B3, respectively (which is significantly smaller than dendra2 Tom20 labelled mitochondria ((853.1 ± 14.70))). A small difference in fragment length is noted between two NS2B3 transfections (mEos-NS2B3 and PAGFP-NS2B3). More cells showing colocalization of NS2B3 complex with mitochondria are given in **Supplementary 4**. Scale bar = 10 μm.

Single-molecule super-resolution microscopy enables such a capability due to its resolution down to a few tens of nanometers and its ability to analyze at a single molecule level. Specifically, the present investigation on dengue provided insights into the formation of single-molecule (NS2B3) clusters, their location, the number of single molecules in a cluster, and their target organelle (here, mitochondrial network) along with its effect (fragmentation of mitochondrial network).

Accordingly, we set on to understand the behavior of these viral proteins (NS2B3 complex) at the single-molecule level. We used super-resolution localization microscopy to understand the distribution of these viral proteins on mitochondria that lead to their fragmentation. We have already established that NS2B3 colocalizes with mitochondria (see, Fig. 2), which is also independently reported in other studies [26] [24]. Taking this as the basis, super-resolution studies were carried out to understand the distribution of viral proteins. Here, we only focus on NS2B3 interaction and its effect on mitochondria. Fig. 4 shows super-resolved images of PAGFP-NS2B3 and mEos-NS2B3 transfected cells along with the respective transfected images. The studies were performed on fixed cells after 48 hours of incubation post-transfection using the standard protocol. We have used point-based clustering technique for analyzing the clusters [41]. One can readily see the appearance of single molecule clusters indicating the formation of NS2B3 clusters. The fact that viral proteins accumulate on the mitochondrial network and form clusters suggests clustering as a precursor that ultimately leads to the fragmentation of the mitochondrial network. Corresponding

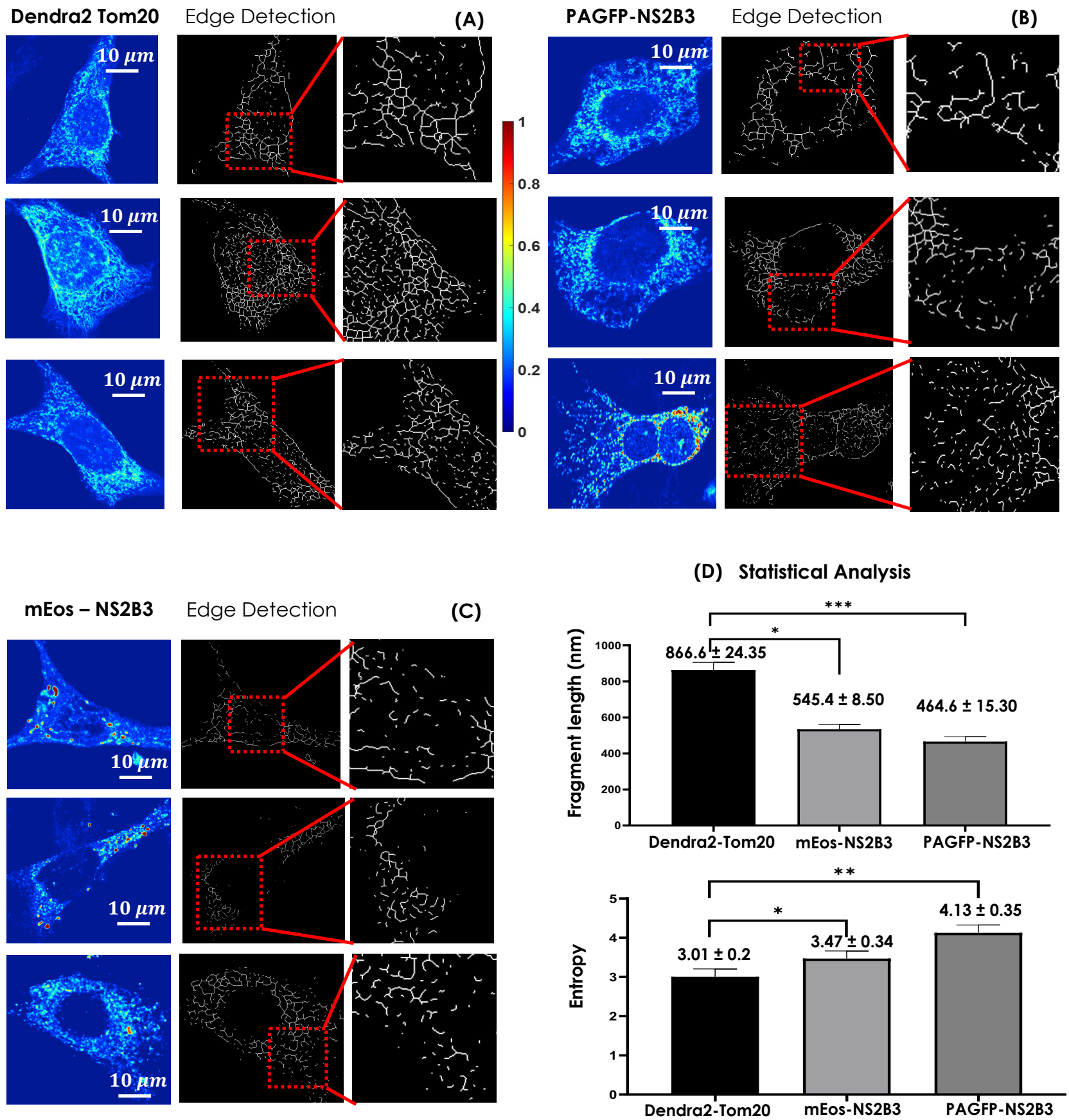

FIG. 3: **Fragmentation study showing shorter mitochondrial fragment effected by NS2B3 protease :** (A) Dendra2-Tom20 transfected NIH3T3 cells along with edge-detection analysis suggests an intact connected mitochondrial network (enlarged sections are also shown). (B,C) Viral plasmid DNA ($PAGFP - NS2B3$ and $mEos - NS2B3$) transfected cells and edge-detection analysis strongly suggests fragmented mitochondrial network. This is better visualized in the enlarged view of selected region. (D) Statistical analysis based on the fragment length indicate an an average decrease in the mitochondrial segment length for $mEos - NS2B3 \sim 545.4 \pm 8.5\ nm$ and $PAGFP - NS2B3 \sim 464.6 \pm 15.3\ nm$ as compared to the control ($Dendra2 - Tom20 \sim 866.6 \pm 24.35\ nm$) with a substantial increase in the fraction of smaller segments. This suggests surge in mitochondrial fragmentation caused by NS2B3 protease. The entropy plot shows an increase in randomness for viral transfected cells ($mEos - NS2B3$ and $PAGFP - NS2B3$) compared to control due to fragmentation of mitochondrial network scattered randomly throughout the cell cytoplasm. We have used one-way ANOVA with the Kruskal-Wallis test for inter-group (cells transfected with different plasmids) statistical comparison. The corresponding statistical significance (P-values) is indicated as, $*\ p < 0.1$, $**\ p < 0.01$, and $***\ p < 0.001$. Estimation of fragment length for NS2B3 transfected NIH3T3 cells and its comparison with empty plasmid Dendra2-Tom20 (no NS2B3) shows significant change with and without the presence of viral protein NS2B3.

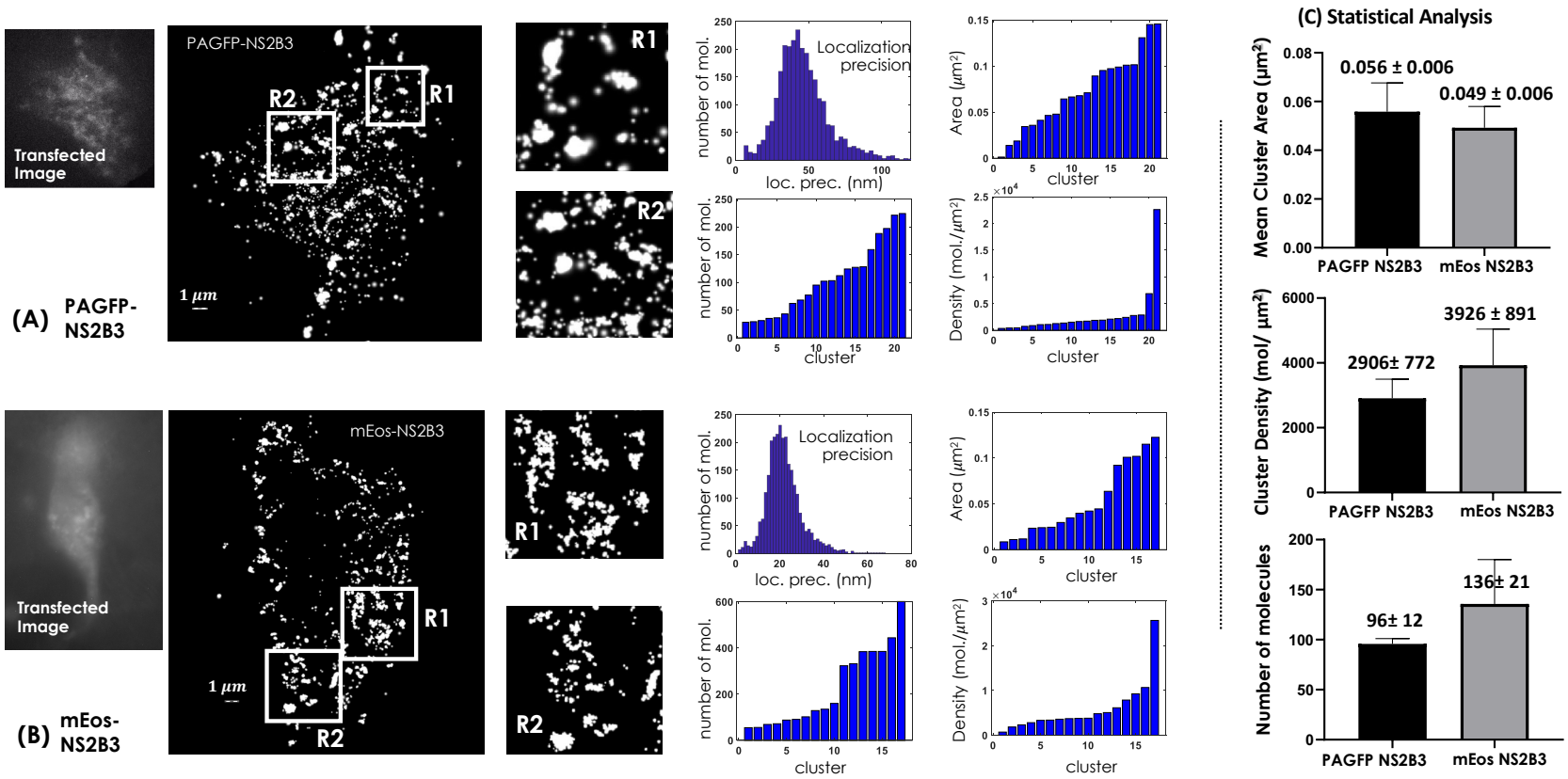

FIG. 4: **Formation of NS2B3 clusters on mitochondrial network:** (A,B) Super-resolution study on the viral plasmid DNA ($PAGFP - NS2B3$ and $mEos - NS2B3$) transfected cells suggests clustering of viral proteins on mitochondrial network. This is further confirmed by enlarged section of selected regions (R1 and R2). The corresponding localization plot indicates an average localization precision of $< 30\ nm$. (C) Statistical analysis shows that the estimated biophysical parameters have an average cluster area of $0.056 \pm 0.006\ \mu m^2$ for PAGFP-NS2B3 and $0.049 \pm 0.006 \mu m^2$ for mEos - NS2B3 respectively. The corresponding cluster density is $2906 \pm 772\ mol/\mu m^2$ and $3926 \pm 891 mol/\mu m^2$ with an average number of 96 ± 12 and 136 ± 21 molecules per cluster for PAGFP-NS2B3 and mEos - NS2B3 respectively. The estimated cluster parameters in cells are transfected with NS2B3 gene indicate the progression of Dengue infection with single-molecule precision. More cells showing NS2B3 cluster formation is given in **Supplementary 5**.

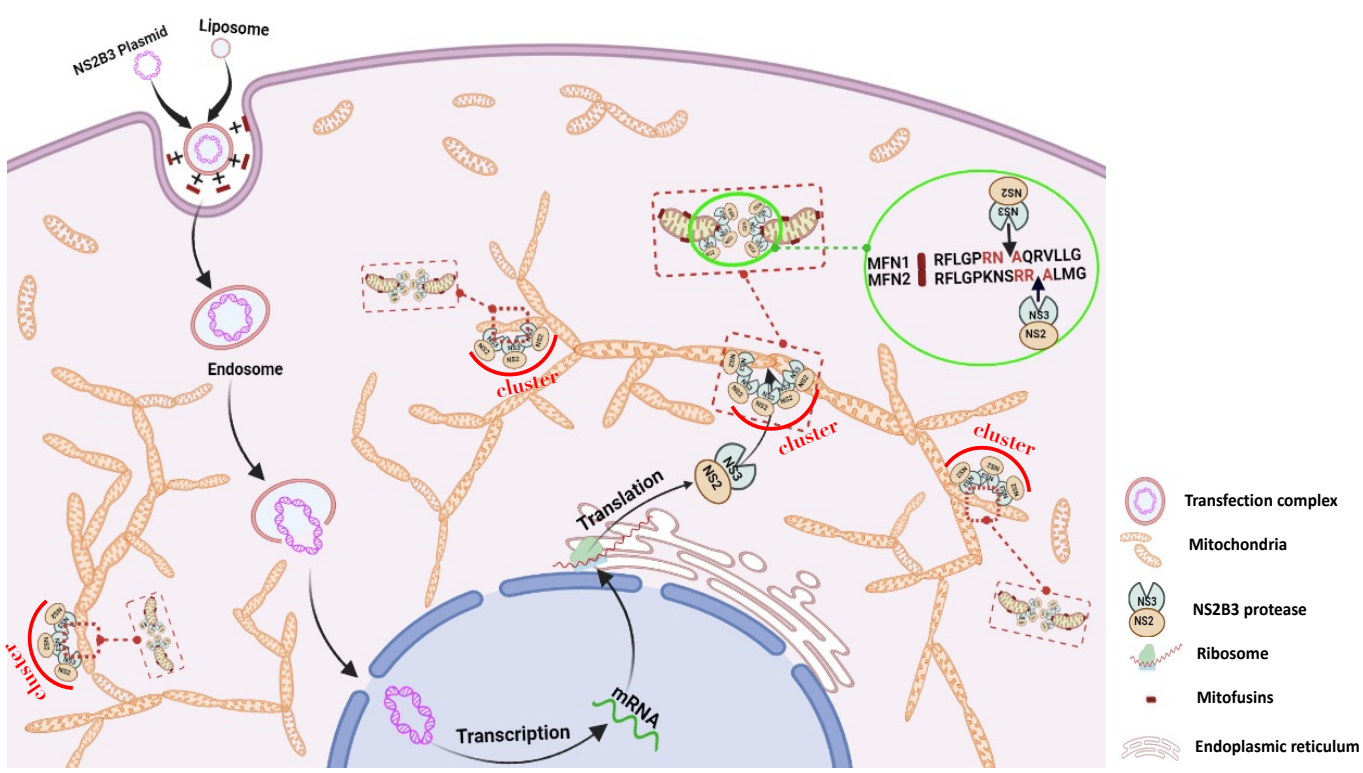

FIG. 5: **The biological mechanism behind NS2B3 induced mitochondrial fragmentation in Dengue:** The experimental evidence suggests entry by endocytosis, followed by uncoating, transcription, translation of the viral complex (NS2B3) [23]. These complex protease are then guided to the mitochondrial network [26]. Subsequently, the complex forms cluster (marked by red semi-circle) and cleaves MF1/2 fusion proteins at GTPase domain (shown by green circle) leading to its disintegration (shown by red dotted box). This cause an avalanche effect leading to the fragmentation of mitochondrial effect, ultimately dismantling its function. All other organelles and proteins are also shown for completeness.

localization precision analysis shows a mean resolution of 20 nm. It is due to the high-resolvability of super-resolution microscopy we are able to see and analyze distinct disconnected viral clusters. Statistical analysis shows a cluster size (Area) of $\approx 0.05\mu m^2$, with a cluster density of $\approx 3500\ mol/\mu m^2$ and an average of $\approx 120\ mol/cluster$. Overall, these biophysical parameters related to viral clustering on the mitochondrial network may have a direct bearing on dengue infection.

We propose the underlying biological mechanism leading to dengue infection based on the limited results and ongoing experiments. Fig. 5 shows the detailed mechanism based on the existing literature and present findings. In our experiment, lipo-complex containing the plasmid enters the cell through endocytosis, followed by uncoating of lipo-complex [39]. Then the plasmid DNA enters the nucleus, and the synthesis of mRNA takes place via the process of transcription [23]. mRNA will be carried to the Ribosomes located on ER followed by translation and post-translation modifications (expression of NS2B3 protease) [23]. The mature protease is then directed to the mitochondrial membrane protein (Mitofusions 1/2) that regulates mitochondrial fusion. The viral complex (NS2B3) forms clusters on the mitochondrial network, and upon reaching a critical number and density, leads to its fragmentation. Specifically, NS2B3 acts on specific sites of mitofusions (the region between coiled-coil domain 1 (HR 1) and the transmembrane domain (TM)), leading to its cleavage. This separates the GTPase domain of mitofusins from coiled-coil domain 2 (HR 2), which leads to its disintegration. This ultimately causes down-regulation of mitofusins lead to mitochondrial fragmentation, and fragmented mitochondria were suggested to induce cell death [26] [47].

Conclusion & Discussion

NS2B3, a protease, acts on the mitochondrial membrane fusion proteins (MFN1/MFN2), leading to its breakdown. Previous studies have shown NS2B3 using innate mitochondrial transport signal (MTS) to get into mitochondrial network [24]. In the present study, we report the accumulation and clustering of the NS2B3 complex on the mitochondrial membrane that leads to the fragmentation of the mitochondrial network. The in-vitro study, using purified proteins, reduced levels of matrix-localized GrpEL1, a cochaperone of mitochondrial Hsp70 (mtHsp70), noticed in NS2B3 expressing dengue infected cells is due to GrpEL1 cleavage [24]. However, in-situ details studies about the biophysical properties of NS2B3 leading to the mitochondrial matrix have not been studied due to the diffraction-limited resolution of existing microscopes. In this study, we used super-resolution microscopy that can decipher details at a single-molecule level to reveal the formation of NS2B3 protein clusters on the mitochondrial network, leading to its fragmentation.

Our study based on single-molecule imaging indicates that the clustering of NS2B3 single molecules occurs at the mitochondrial matrix. Further, transient-transfection and protein import studies demonstrate that having a critical number ($\geq$ 120) is essential for cleaving the mitochondrial network. Additionally, a relatively large number of short fragments of the matrix ($464.6 \pm 15.3\ nm$ for PAGFP-NS2B3 and $545.4 \pm 8.50\ nm$ for $mEos - NS2B3$ transfected cells) was observed in NS2B3 expressing cells, compared to long-sized fragments ($866.6 \pm 24.35\ nm$) in control ($Dendra2 - Tom20$). (Figure 3). Super-resolution microscopic study and associated statistical analysis estimated critical values for the biophysical parameters (cluster size (Area) of $\approx 0.05\ \mu m^2$, cluster density of $\approx 3500 mol/\mu m^2$ and an average of $\approx$ 120 $mol./cluster$) that are essential for the mitochondrial fragmentation initiation in NS2B3 transfected cells. These parameters are critical for determining the overall progress of viral infection and, specifically, the role of the NS2B3 complex during actual Denv-2 viral infection. This is possible due to super-resolution microscopy's capability, which can determine biological mechanisms down to single molecule precision.

The clustering of the viral complex is a prerequisite for the fragmentation of the mitochondrial network. Previous studies have indicated that NS3 complex-induced cleavage of GrpEL1, a matrix protein is a major cause of mitochondrial matrix fragmentation [24]. GrpEL1 cochaperones are essential for the activity of mtHsp70, which is involved in various functions such as protein import, folding, redox homeostasis, and Fe-S cluster biogenesis [42]. During the early phase of dengue infection, GrpEL2 partially replaces the functions of GrpEL1. However, NS2B3 protease causes depletion of GrpEL1 that lead to dysfunctional mitochondria [43], ultimately taking over mitochondrial machinery critical roles in the cells, such as innate immunity [44], apoptosis [44], cellular metabolism [45], and aging [46] to favor viral production. Moreover, Yu et al. (2015) have shown the association of NS2B3protease with mitochondrial membrane [26]. Although more direct evidence may be necessary to establish the mechanism, the basic understanding of clustering can be of the therapeutic potential that may be exploited to design new drug targets or may help explore existing FDA-approved drugs. Specifically, any drug candidate that can intervene in the process of viral clustering or reverse it may be an effective strategy to stop/contain severe dengue infection with the hope that the immune system will take rest care.

III. MATERIALS & METHODS

A. Recombinant Plasmids

Recombinant plasmid PAGFP-NS2B3 was generated by subcloning of NS2B3 protease from pcDNA-DENV2-NS2B3, a Gift from Alan Rothman [30] at Pst1- BamH1 site of PAGFP C1 plasmid, a gift from Jennifer Lippincott-Schwartz [31]. NS2B3 protease with PstI-BamHI overhangs were generated by PCR using NS2B3-specific oligonucleotide primers, NSPstFP with Pst 1 site as forward primer and NSBamRP with Bam H1 site as reverse primer. Recombinant plasmid pmEos_NS2B3 was generated by subcloning of mEos fragment from mEos3.2-TOMM20-N-10, a gift from Michael Davidson [32] at Nhe I- Pst I site of PAGFP-NS2B3 by removing PAGFP fragment. mEos with NheI-PstI overhangs were generated by PCR using oligonucleotide primers, mEosNheFP with Nhe 1 site as forward primer mEosPstRP with Pst 1 site as reverse primer. The list of the sequence of primers used are given in Table 1. PCR was performed using Phusion™ High-Fidelity DNA Polymerase (Thermo Fisher Scientific, India). All restriction enzymes used were purchased from Thermo Fisher Scientific, India. Subcloning and transformation were performed using the standard protocol (Sambrook and Russel, 2001). The recombinant plasmids, both PAGFP-NS2B3, and mEos-NS2B3 were used to transfect 3T3 cells (mouse embryonic fibroblast cell line) to study the interaction of dengue NS2B3 with the cell organelles.

B. Cell Line and Transfection

The recombinant plasmids, both PAGFP-NS2B3, and mEos-NS2B3 were used to transfect 3T3 cells (mouse embryonic fibroblast cell line) to study the interaction of dengue NS2B3 with the cellular organelles. The cells used in this study were obtained from our collaborator Dr. Upendra Nongthomba (Biological Sciences, Indian Institute of Science, Bangalore, India). Transfection was performed using 1µg of plasmid DNA with Lipofectamine 3000 (Invitrogen, USA) according to manufactures instructions. The cells were cultured on a coverslip (No.0) (Blue star, India) in a 35mm dish with a density of 10^5 cells/ml. After 12h incubation cells were transfected with respective plasmids. Cells transfected with Dendra2-Tom20 were used as control. After 48 h of post-transfection cells were washed twice with 1X PBS, and cells were incubated fixed with 3.7% (W/V) paraformaldehyde for 15 min. It was followed by washing with 1X PBS two times. Cover slip was removed from the 35mm dish and placed on a clean slide with mounting media fluorosave (Thermofisher, USA). The Fixed cells were made airproof by applying nail paint on the edges for long time preservation and further investigation.

TABLE I: **List of primers used for subcloning protein of interest (NS2B3) and the marker proteins (PAGFP & mEos3.2).**

No.	Primer Name	Sequence (5'.....3')
1	NSPstFP	AACTGCAGTCATGGCAAGCTGGCC
2	NSBamHRP	ATGGATCCACCGGTACGCGTAGAATCG
3	mEosNheIFP	CTAGCTAGCCATGAGTGCGATTAAGCC
4	mEosPstIRP	GTTCTGCAGTTCGTCTGGCATTGTCAG

C. Image acquisition using confocal microscopy and data processing

Fixed samples were imaged in Zeiss LSM 510 inverted microscopy (confocal microscopy Leica SP8, Indian Institute of Science, Bangalore, India) using 63 X oil immersion objective. The cells were illuminated with a 488nm Laser (argon Multiline), and the emission was captured beyond 510nm by using a long pass filter and band pass filter and using a 1 Airy unit pin hole. Both the samples (PAGFP-NS2B3 and mEos-NS2B3) were illuminated using a 488 nm laser. The images obtained from confocal microscopy were skeletonized using image J [33]. The skeletonized image was then processed using a script written in MATLAB. The length of each fragment (branches are not involved in counting) was measured and then the statistical analysis was performed. Entropy measures the randomness of the signal in the image. We have calculated the Entropy of Recombinant plasmid and Control (Dendra2-Tom20). Entropy is defined as

$$Entropy = -\sum p * log_2 p \tag{1}$$

where p contains the normalized histogram counts

D. Co-localization studies of mitochondria using Mito tracker orange and recombinant NS2B3

Mitotracker orange is a dye that selectively labels mitochondria by reacting with the thiol group of cysteine residues. Then it gets accumulated in the mitochondrial matrix. Mito tracker orange (Invitrogen, USA) was dissolved in DMSO to obtain 1mM stock solution. The stock solution was diluted in DMEM to get a working concentration of 175nm, was used for staining. Cells transfected with PAGFP-NS2B3 and mEos-NS2B3 for 48 hrs and then stained with $175nM$ mitotracker orange followed by incubation for 1h 15 min at 37^oC with 5% CO2. It was followed by fixing and preservation as described above. The fixed samples were imaged in confocal microscopy using two colors. We imaged PAGFP-NS2B3 and mEos-Tom20 using 488nm wavelength, and Mito-tracker was imaged using a 561nm wavelength laser. The images captured were optically zoomed three times to focus on only one or two cells and then they were colocalized. The co-localization of images is done using Leica software, and Pearson coefficients for the colocalized image were calculated. The colocalized image is indicated by the yellow color as shown in image 2(C). The Pearson coefficient of more than 85% shows the colocalization of recombinant NS2B3 with mitochondria.

E. Super-resolution imaging for Single-molecule analysis

Transfected cells (PAGFP-NS2B3 and mEos-NS2B3) were fixed, and super-resolution studies were carried out. We used a 405 nm laser for the activation of the samples and 488nm and 561 nm lasers were used for PAGFP-NS2B3 and mEos-NS2B3, respectively. The transfected cells were seen by 470-490 nm blue light. The system is a homemade system [40] It is seen after reconstructing the super-resolution image that NS2B3 forms the clusters, so we further investigated the cluster area, number of molecules and density of clusters. The cluster analysis was done using the point-based clustering algorithm [41].

F. Statistical Analysis

All the statistical analyses were performed using GraphPad Prism 8. Data for statistical analysis were copied directly from Matlab files. Statistical significance between the test group and control were calculated by a nonparametric t-test. The mitochondrial branch lengths of control (dendra2 tom20) and samples (PAGFP-NS2B3 and mEos-NS2B3) were considered as same (null hypothesis). From the t-test distribution table, p-value is determined for the calculated t-value. If the obtained p value is less than 0.05, it leads to the rejection of the null hypothesis and indicates the significant difference between the control and the sample. However, for comparing more than two groups, we have used one-way ANOVA with the Kruskal-Wallis test. The corresponding statistical significance (P-values) is indicated as, $*\ p < 0.1$, $**\ p < 0.01$, $***\ p < 0.001$, and $****\ p < 0.0001$. The statistical analysis is based on a total of 15 cells from 3 separate experiments for each group.

Acknowledgements: The authors acknowledge ICMR postdoctoral fellowship to JMV. The authors thank Dr. Subhra Mondal (University of Nebraska - Lincoln, USA) for rigorously going through the manuscript and providing valuable inputs.

Data Availability: The data that support the findings of this study are available from the corresponding author upon request.

Supplementary Info: The manuscript is supported by supplementary material (Supplementary 1- 5) .

Disclosures: The authors declare no conflicts of interest.

[1] N. J. Barrows et al., Biochemistry and Molecular Biology of Flaviviruses, Chem. Rev. 118, 4448–4482 (2018).
[2] B. D. Lindenbach et al., Flaviviridae: the viruses and their replication, Fields Virology 1, 1101–1152 (2007).
[3] T. J. Chambers et al., Flavivirus Genome Organization, Expression, and Replication, Annu. Rev. Microbiol. 44, 649–688 (1990).
[4] B. D. Lindenbach et al., Flaviviridae, 1, 712–746 (2013).
[5] R. Perera and R. J. Kuhn, R. J Structural proteomic of dengue virus. Curr. Opin. Microbiol. 11, 369-377, (2008).
[6] P. Erbel et al.Structurral basis for the activation of flaviviral NS2B3 protease from dengue and west nile virus. Nat. Struct. Mol. Biol. 13, 372-373 (2006).
[7] Aleshin et.al. Structural evidence for regulation and specificity of flavi viral protease and evolution of flavi viridae fold. Protein Sc. 16, 795-806 (2007).
[8] D. Lamarre et al., An NS3 protease inhibitor with antiviral effects in humans infected with hepatitis C virus, Nature 426, 186–189 (2003).
[9] E. M. Silva et al., Dengue virus nonstructural 3 protein interacts directly with human glyceraldehyde-3-phosphate dehydrogenase (GAPDH) and reduces its glycolytic activity, Sci. Rep. 9, 2651 (2019).
[10] G. Wengler and G. Wengler, The NS 3 nonstructural protein of flaviviruses contains an RNA triphosphatase activity, Virology 197, 265–273 (1993).
[11] T. Cui, et al., Recombinant Dengue Virus Type 1 NS3 Protein Exhibits

Specific Viral RNA Binding and NTPase Activity Regulated by the NS5 Protein, Virology 246, 409–417 (1998).
[12] D. Leung et al., Activity of Recombinant Dengue 2 Virus NS3 Protease in the Presence of a Truncated NS2B Co-factor, Small Peptide Substrates, and Inhibitors. J. Biol. Chem. 276, 45762–45771 (2001).
[13] C. Nitsche et al. Biochemistry and medicinal chemistry of dengue virus protease. Chem. Rev. 114, 11348-11381 (2014).
[14] T. C. Pierson and M. S. Diamond, The continued threat of emerging flaviviruses, Nature Microbiol. 5, 796–812 (2020).
[15] Y. Li et al., Membrane topology of NS2B of dengue virus revealed by NMR spectroscopy, BBA - Biomembranes 1848, 2244–2252 (2015).
[16] Y. Li et al., Secondary structure and membrane topology of dengue virus NS4B N- terminal 125 amino acids, BBA – Biomembranes 1848, 3150–3157 (2015).
[17] Y. Li et al., Secondary Structure and Membrane Topology of the Full-Length Dengue Virus NS4B in Micelles, Angew. Chem. 128, 12247–12251 (2016).
[18] Y. Chen et al., Dengue virus infectivity depends on envelope protein binding to target cell heparan sulfate, Nat. Med. 3, 866–871 (1997).
[19] A.L. Byk and A.V. Gamarnik, Properties and Functions of the Dengue Virus Capsid Protein, Annual Review of Virology 3,1, 263-281 (2016).
[20] D. J. Gubler, Emerging vector-borne flavivirus diseases: are vaccines the solution, Expert Rev. Vacc. 10, 563–565 (2011).
[21] N. S. Heaton et al., Dengue virus nonstructural protein 3 redistributes fatty acid synthase to sites of viral replication and increases cellular fatty acid synthesis, Proc. Natl. Acad. Sci. (USA) 107, 17345–17350 (2010).
[22] I. M. Yu et al., Structure of the immature dengue virus at low pH primes proteolytic maturation, Science 319, 1834–1837 (2008).
[23] L. Li et al., The flavivirus precursor membrane-envelope protein complex: structure and maturation, Science 319, 1830–1834 (2008).
[24] C. Gandikota et al., Mitochondrial Import of Dengue Virus NS3 Protease and Cleavage of GrpEL1, a Cochaperone of Mitochondrial Hsp70, J. Virol. 94, e01178-20 (2020).
[25] W. Reidl et al., Zika Virus NS3 Mimics a Cellular 14-3-3-Binding Motif to Antagonize RIG-I- and MDA5-Mediated Innate Immunity, Cell Host Microbe . 26, 493-503 (2019).
[26] C. Y. Yu et al., Dengue Virus Impairs Mitochondrial Fusion by Cleaving Mitofusins, PLoS Patho. 11(12), 1-24 (2015).
[27] L. Galluzzi et al., Mitochondria: master regulators of danger signaling, Nat. Rev. Mol. Cell Biol.13, 780–788 (2012).
[28] L. Chatel-Chaix et al., Dengue Virus Perturbs Mitochondrial Morphodynamics to Dampen Innate Immune Responses, Cell Host Microbe 20, 342-356 (2016).
[29] I.S. Kim et al., Mitofusin 2, a key coordinator between mitochondrial dynamics and innate immunity, Virulence, 12 2273-2284 (2021).
[30] addgene plasmid #115906 $http://n2t.net/addgene:115906; RRID: Addgene_115906$
[31] addgene plasmid #11910 $http://n2t.net/addgene:11910; RRID: Addgene_11910$
[32] Addgene plasmid#57483; $http://n2t.net/addgene:57483; RRID: Addgene_57483$
[33] J. Schindelin et al. Fiji: an open-source platform for biological-image analysis. Nat Methods 9, 676–682 (2012).
[34] J.F. Sambrook and D.W. Russell, Molecular Cloning: A Laboratory Manual (3rd ed.), Cold Spring Harbor Laboratory Press (2001).
[35] S. Samanta et al., Fluorescent Probes for Nanoscopic Imaging of Mitochondria, Chem 5, 1697–1726, (2019).
[36] S. Kanaji et al., Characterization of the signal that directs Tom20 to the mitochondrial outer membrane, Cell. Biol . 151, 277-288 (2000).
[37] M. M. Win et al., Ultrastructural features of human liver specimens from patients who died of dengue hemorrhagic fever, Trop. Med. Infec. Dis. 4, 1-13 (2019).
[38] B. Singh et al., Defective Mitochondrial Quality Control during Dengue Infection Contributes to Disease Pathogenesis. Virology 96, 1-29 (2022).
[39] A. K. Parker et al., Nonviral Gene Delivery: Techniques and Implications for Molecular Medicine. Expert Rev. Mol. Med. 5, 1-15 (2003).
[40] Joshi P et al., Adaptable single molecule localization microscopy (aSMLM) for superresolution optical fluorescence imaging, Appl. Phys. Lett. 119, 173703 (2021)
[41] P. Joshi and P. P. Mondal, Single-Molecule Clustering for Super-Resolution Optical Fluorescence Microscopy. Photonics 9, 7 (2022).
[42] D. J. Naylor et al., Evidence for the existence of distinct mammalian cytosolic, microsomal, and two mitochondrial GrpE-like proteins, the Co-chaperones of specific Hsp70 members, J Biol Chem. 273, 21169-21177 (1998).
[43] A. Marada et al., Mge1, a nucleotide exchange factor of Hsp70, acts as an oxidative sensor to regulate mitochondrial Hsp70 function, Mol Biol Cell . 24, 692-703 (2013).
[44] S. E Weinberg et al., Mitochondria in the regulation of innate and adaptive immunity, Immunity 42, 406-417 (2015).
[45] J . B. Spinelli and M. C. Haigis, The multifaceted contributions of mitochondria to cellular metabolism, Nat. Cell Biol . 20, 745-754 (2018).
[46] A. Bratic and N. G. Larsson, The role of mitochondria in aging, J Clin Invest. 123, 951-7 (2013).
[47] M. E. Henriques and M. Joaquim, Mitofusins: Disease Gatekeepers and Hubs in Mitochondrial Quality Control by E3 Ligases, Front. Physiol. 10, 517, (2019).
[48] A. Horn et al., Mitochondrial fragmentation enables localized signaling required for cell repair, J. cell biol. 219, 5, e201909154 (2020).
[49] A. Nasonovs et al., A549 cells contain enlarged mitochondria with independently functional clustered mtDNA nucleoids, Plos One 16, 3, e0249047 (2021).
[50] Y. Zhang et al., Mitoguardin Regulates Mitochondrial Fusion through MitoPLD and Is Required for Neuronal Homeostasis, Mol Cell 61, 111-24 (2016).
[51] C. S. Palmer et a., Super-resolution microscopy reveals the arrangement of inner membrane protein complexes in mammalian mitochondria, J Cell Sci 134, jcs252197 (2021).
[52] M. Bhagawati et al., The receptor subunit Tom20 is dynamically associated with the TOM complex in mitochondria of human cells, Mol. Biol. Cell 32, 1-11 (2021).
[53] M. Yano et al., Functional Analysis of Human Mitochondrial Receptor Tom20 for Protein Import into Mitochondria, J. Biol. Chem. 273, 26844-26851 (1998).
[54] A. Zahedi et al., Deep Analysis of Mitochondria and Cell Health Using Machine Learning, Sci. Rep. 8, 16354 (2018).